

# Relaxation Fluctuations in Quantum Chaos

Arul Lakshminarayan\*

*Physical Research Laboratory, Navarangapura, Ahmedabad, 380009, India.*

(February 5, 2008)

Classically chaotic systems relax to coarse grained states of equilibrium. This article reports work on quantized bounded relaxing systems, in particular the quasi-periodic fluctuations associated with the correlation between two density operators, whose classical limits as phase space partitions is evident. These fluctuations can distinguish classically chaotic and regular motions, thus providing a novel diagnostic devise of quantum chaos. We uncover several features of the relaxation fluctuations that are shared by disparate systems thus establishing restricted universality. The universal form of these fluctuations for generic quantized chaotic systems with time reversal symmetry is worked out within the framework of Random Matrix Theories and is found to be consistent with the numerical simulations performed on varied systems.

To appear in the proceedings of the conference on “*Nonlinear Dynamics and Computational Physics*” held at Physical Research Laboratory, Ahmedabad, in Nov. 1997.

## I. INTRODUCTION

Classical dynamical systems have been classified into a hierarchy of deterministic randomness. We have well studied examples from integrable systems to Bernoulli systems, from the regular to those that are in a coarse grained manner identical to stochastic processes. An important notion in this context is that of mixing, as exemplified in the now classic coke-rum mixture of Arnold and Avez [1]. Apart from the fundamental role it plays in deterministic randomness, alias chaos, it is the backbone of the foundations of classical statistical mechanics. While ergodicity is compatible with equilibrium, it is mixing that would ensure the drive to this state. The role of deterministic chaos in statistical mechanics is under active research, for instance it is not clear that thermal equilibrium is the result of only deterministic chaos or whether large system sizes are a necessity.

Low dimensional completely chaotic classical systems are however characterized by “equilibrium states” as the underlying invariant densities and mixing drives sufficiently well behaved initial states to this equilibrium. This affords the evaluation of averages much the same way as in equilibrium statistical mechanics. On the introduction of quantum mechanics however, the picture is not quite so clear even for low dimensional systems. The phenomenon of quantum suppression of classical chaos in diffusive systems is now well studied, and several localization mechanisms have been put forward which inhibit quantum mixing [3], yet the issues in the situation of “hard chaos” for bounded chaotic systems relaxing to an equilibrium have not been sufficiently addressed.

This paper studies quantum objects that are obviously connected to the twin issues of ergodicity and mixing in the classical limit. In the process we use models having a discrete spectra whose classical limit is known to be chaotic. The most convenient for our purposes is the quantization of two dimensional area preserving maps on the torus- a much studied subject. The Hilbert space is then finite dimensional and we have fully all the contradictions between quantum and classical chaos, while retaining the attractive feature of being able to do the quantum mechanics up to machine precision and size.

Let the relevant classical phase space be  $\Omega$ . This could be for instance the energy shell on which the Hamiltonian flow is restricted. We may formulate mixing either in terms of phase space functions or densities. Let  $A$  and  $B$  be two subsets of the phase space such that they do not intersect. Let  $\chi_A(x)$  and  $\chi_B(x)$  be the two characteristic functions of these subregions. Let the flow integrated for a time  $t$  be denoted by  $f^t$ , this could be a continuous flow or a discrete map, we formulate this for the case of maps in which case  $t$  is an integer. The invariant measure of the flow is denoted by  $\mu$ , in the present context of area preserving maps this is simply the physical area of the phase space region.

The central quantity of interest is the correlation between the functions  $\chi_A$  and  $\chi_B$ . In more graphic language, as the subregion  $A$  evolves with the motion the correlation is the fractional area of its intersection with the region  $B$ . If in the long time limit this factorises into the fraction of the areas of  $A$  and  $B$  we have mixing. In other words the fraction of  $A$  systems in  $B$  is the fractional area of  $B$  in the long time limit.

$$\mu(f^t(A) \cap B)/\mu(A) \longrightarrow \mu(B)/\mu(\Omega) \quad (1.1)$$

Mixing systems are a step above ergodic ones in the hierarchy of classical dynamical systems. Ergodicity is the equality of the time average and phase space average of almost all points in the phase space. This can also be formulated as decorrelation on the average. Thus a system is ergodic if

$$\lim_{T \rightarrow \infty} \frac{1}{T} \sum_{t=1}^T \mu(f^t(A) \cap B)/\mu(A) = \mu(B)/\mu(\Omega). \quad (1.2)$$

Classical mixing systems are characterized by a series of complex numbers or resonances that dictate the rate of decay of correlations. Thus for purely hyperbolic or Axiom A systems we can write

$$\mu(f^t(A) \cap B)/\mu(A) - \mu(B)/\mu(\Omega) = \sum_i C_i \exp(\lambda_i t). \quad (1.3)$$

The  $\lambda_i$  ( Ruelle resonances ) are in general complex numbers with negative real parts independent of the particular partitions  $A$  and  $B$ . Explicit calculation of these resonances is a challenging part of dynamical systems theory; there

are special models which are isomorphic to finite Markov processes for which these can be analytically found; for example the multi-baker maps [4,5].

What we wish to study below are quantities in quantum mechanics that are naturally related to the classical correlation functions defined above. These are of course correlations between operators and when the dynamics is classically chaotic we expect the quantum correlations to also “decay” in some sense. Since we will consider systems with discrete spectra this does not strictly happen and eventually there are oscillations. We will characterize these oscillations and show that when the dynamics is classically chaotic they are well predicted by Random Matrix Theory (RMT).

## II. THE QUANTUM CORRELATION FUNCTION

The relevant dynamical space on quantization is a Hilbert space  $H_N$ . For regions of phase space we consider subspaces of the Hilbert space. Since we have in mind classical maps on the two torus, let the Hilbert space be of finite dimensionality  $N$ . Let there be two distinct density operators on  $H_N$  (may or may not be projection operators),  $P_A$  and  $P_B$ . We will study the cases when these operators on  $H_N$  have obvious classical limits as functions on the phase space. We will restrict ourselves initially, and largely, to the case when the operators are projection operators such that  $P_A + P_B = I_N$ , where  $I_N$  is the  $N$  dimensional identity matrix. Classically this corresponds to choosing the partitions  $A$  and  $B$  such that  $A \cup B = \Omega$ .

We sidestep the question of assigning an operator to a general subregion of phase space, and whether this is possible at all (say through the Wigner-Weyl transform of the characteristic function), by restricting this study to particularly simple subspaces (or density operators) both of  $\Omega$  and on  $H_N$  and going from the quantum to the classical instead of vice versa. Choosing an “arbitrary” subspace (or operator) of  $H_N$  obviously does not correspond to a proper subregion of the classical phase space and we will see that such subspaces do not provide interesting relaxation behaviors in that they do not distinguish between classically chaotic and regular motions.

If we use pure states, say  $|n\rangle$ , we can construct the density operators as  $\sum |n\rangle\langle n|$ . Let the dimensionality of the subspace  $A$  be  $n_A = f_A N$ ; then  $n_B = N - n_A = f_B N$ . The fractions  $f_A$  and  $f_B$  determine the relative sizes of the partitions. We will mostly use projection operators that are diagonal in the position basis. In this case the classical region corresponding to

$$P_A = \sum_{n=0}^{f_A N - 1} |n\rangle\langle n| \quad (2.1)$$

is the rectangle  $[0, f_A) \times [0, 1)$  and the region corresponding to  $P_B$  is the rectangle  $[f_A, 1) \times [0, 1)$ , as the phase space is taken to be the unit torus  $(q, p) = [0, 1) \times [0, 1)$ .

The dynamics is an unitary operator  $U$  acting on the states of  $H_N$ . The central quantity of interest is then

$$C_{AB}(t) = \text{Tr}(U^t P_A U^{-t} P_B) / N, \quad (2.2)$$

which gives us the overlap of the subspace  $A$  propagated for time  $t$  with the subspace  $B$ . We may note that this is an important and natural physical quantity to study and has appeared before in several contexts, for example ref. [6]. It can also be viewed as an analogue of Landauer conductance for bound systems and as such should be of considerable importance in quantum transport. If in fact there is factorization in time then  $C_{AB}(\infty)$  must be compared with  $\text{Tr}(P_A)\text{Tr}(P_B)/N^2 = f_A f_B$ .

Since  $U$  has a discrete and finite spectrum, the correlation can only be a finite sum of purely oscillatory terms and can therefore display decay only over short time scales (of the order of Heisenberg time). The decorrelation is therefore not expected. As an extreme example if we consider the case when the projection operators are constructed out of the basis functions of  $U$  the correlation is zero for all time. This is an extreme case and for instance it is not clear what the classical limit is of the Wigner-Weyl transform of projection operators constructed out of such a basis. We will consider “generic” subspaces and projection operators and any claim of universality made below has to

be viewed with this caveat. We may note that this plagues Random matrix theory descriptions of eigenfunctions as well, as it involves basis dependent quantities. Here the basis dependence enters as the basis in which the projection operators are diagonal.

It was suggested earlier using quantized multi-baker maps that the quantum correlation function approached the classical correlation function in the classical limit corresponding here to  $N \rightarrow \infty$  [7]. Certain remarkable features of quantum relaxation were noted there including relaxation localization and effects of symmetries on transport. Here we wish to study the fluctuation properties more closely and uncover possible universal features. Therefore we study rather standard models like the Taylor-Chirikov (standard) map [3], the kicked Harper system [10] and the baker map [11] qalthough most of these models do not have explicit expressions for the classical Ruelle resonances and are probably not Axiom A systems (except the baker map). However it is very reasonable to assume that in certain well known parameter regimes they can be for all practical purposes mixing systems.

Normalizing the correlation so that the classical limit, if it exists, is for large times unity we study the quantity  $c(t) = C_{AB}(t)/f_A f_B$ , where from now we will acknowledge implicitly the dependence of the correlation on the particular choice of partitions. Fig. 1 shows an example of the generic behaviour of  $c(t)$ , this particular data being for the standard map at two different values of the inverse Planck constant  $N$  for the same classical value of the chaos parameter. The initial relaxing behaviour is not clear from the figures as the time scales are much larger than the inverse of the principal Ruelle resonance. The projection operators used are diagonal in the discrete position basis,  $P_A$  is given by Eq.( 2.1) and  $P_B = I_N - P_A$ . The position eigenbasis is denoted as  $|n\rangle$  and in this figure  $f_A = f_B = 1/2$ .

We have used dimensionless scaled position and momentum co-ordinates and time is measured as multiples of the period of the kick, taken as unity. Modulo one conditions restrict the phase space to the unit torus so that the dimension of the Hilbert space  $N$  is related to the Planck constant as  $N = 1/h$  and the classical limit corresponds to  $N \rightarrow \infty$  while the parameters of the map such as the kick strengths are scaled and dimensionless.

The first observation is that the quantum correlation is in fact quite close to the classical value of unity, second is that the average of the oscillations in relation to unity will give us some information about whether quantum mechanics is inhibiting transport or otherwise, thirdly this average must in the classical limit tend to unity, fourth is the observation that the fluctuations are getting smaller in the classical limit and must tend to zero. Some of these observations have been made and substantiated earlier [7,8], here we will elaborate and present more results.

Previous work on the use of time developing states to study the quantum manifestations of chaos have basically concentrated on the survival probability of a pure state [9]. This corresponds to the choice  $P_A = P_B = |\psi\rangle\langle\psi|$  with an arbitrary normalized initial state  $|\psi\rangle$  and thus  $f_A = f_B = 1/N$ . Such survival probabilities averaged over random initial states show a distinct difference between chaotic and regular systems. In contrast what we study in this paper are density (or projection) operators and not pure states. It becomes quite important that  $f_A N$  and  $f_B N$  are large and are of the order of the Hilbert space dimensionality  $N$  itself. Besides any “arbitrary” state can be chosen for the calculation of the survival probability while we will restrict ourselves to those projection operators that can be interpreted as phase space regions in the classical limit. This is to ensure that the classical transition to chaos is fully reflected in the quantum relaxation, as will be illustrated below.

### III. THE FLUCTUATION PROPERTIES

The quantum “equilibrium” as opposed to the classical is an highly oscillatory state, with the fluctuations coming from the discrete nature of the spectrum. We will denote the time average of the correlation function by  $\langle c \rangle$  and its variance by  $\sigma^2$ . These quantities can be written in terms of the eigenfunctions of the evolution operator  $U$ , which satisfy the following equation.

$$U|\psi_m\rangle = e^{iE_m}|\psi_m\rangle \quad m = 0, \dots, N-1 \quad (3.1)$$

The real numbers  $E_m$  are the eigenangles of the quantum map, and we are assuming that there are no exact degeneracies as is the generic case. The correlation is then

$$c(t) = \frac{1}{Nf_A(1-f_A)} \sum_{m_1, m_2} \sum_{n_1=0}^{Nf_A-1} \sum_{n_2=Nf_A}^{N-1} e^{it(E_{m_2}-E_{m_1})} \langle n_2 | \psi_{m_1} \rangle \langle \psi_{m_1} | n_1 \rangle \langle n_1 | \psi_{m_2} \rangle \langle \psi_{m_2} | n_2 \rangle \quad (3.2)$$

Thus we can express the average quite simply as

$$\langle c \rangle = \frac{1}{Nf_A(1-f_A)} \sum_{m=0}^{N-1} \sum_{n=0}^{f_A N-1} \sum_{n'=f_A N}^{N-1} |\langle n | \psi_m \rangle|^2 |\langle n' | \psi_m \rangle|^2. \quad (3.3)$$

Thus the average is a measure of the distribution of the eigenvectors in the subspaces  $A$  and  $B$ . We suggest that  $\langle c \rangle < 1$  generically, indicating a certain reluctance to participate equally in both the partitions in proportion to their sizes. A quantity of natural interest is the variance of the fluctuations which exist irrespective of the symmetries of the system. This can also be expressed in terms of the eigenfunctions of the system. In the particular case when  $P_A + P_B = I_N$ , writing for  $f_A$  simply  $f$ , we get after some simplifications

$$\sigma^2 = \frac{2}{N^2 f^2 (1-f)^2} \sum_{m_2 > m_1} \left| \sum_{n=0}^{fN-1} \langle n | \psi_{m_2} \rangle \langle \psi_{m_1} | n \rangle \right|^4. \quad (3.4)$$

Thus the variance measures a correlation between distinct pairs of eigenfunctions. There is a coherent partial sum over  $Nf$  states that makes the variance non-trivial.

## A. The Models

Apart from time reversal symmetry there may be phase space symmetries that are either preserved or not in the quantum mechanical models. The results in [8] are for the case when there is an additional phase space symmetry present which is reflected quantally as a parity symmetry of the eigenfunctions. This being a special (but important) case we continue our study here for the more generic case when the eigenfunctions possess no symmetries. Then the only important symmetry is that of time reversal.

The Taylor-Chirikov, or the standard map, or the kicked rotor, used in this paper is described below [3,15]. Let the classical map be  $(q_{t+1} = q_t + p_{t+1}, p_{t+1} = p_t - V'(q_{t+1}))$ , both  $q$  and  $p$  taken mod 1.  $V'$  is the derivative of the kicking potential which is assumed to have unit periodicity. The toral states are assumed to satisfy certain boundary conditions specified by a point on the dual torus. Let  $|q_n\rangle$  and  $|p_m\rangle$  be the position and momentum states then  $|p_{m+N}\rangle = e^{-2\pi i a} |p_m\rangle$  and  $|q_{n+N}\rangle = e^{2\pi i b} |q_n\rangle$ , where  $(a, b)$  are real numbers between 0 and 1;  $N$  is the dimensionality of the Hilbert space. If  $b = 0$ , upon canonical quantization we get the finite unitary operator

$$U_{n,n'} = \frac{e^{i\pi/4}}{\sqrt{N}} \exp(-2\pi i N V(\frac{n+a}{N})) \exp(i \frac{\pi}{N} (n - n')^2). \quad (3.5)$$

We have used for the standard map  $V(q) = K \cos(2\pi q)/(2\pi)$ , and  $a = 1/2$  makes the quantum map possess an exact parity symmetry about  $q = 1/2$ . Thus we break the symmetry by simply choosing different boundary conditions for the wavefunctions. If  $b \neq 0$  then time reversal symmetry is also broken. Therefore there are two classes of models with no special wavefunction symmetries. We call the case  $(a = 1/2, b = 0)$  the symmetric standard map. The values of  $N$  are restricted to the even integers.

The kicked Harper map [10] on the torus is similar to the above system except for the momentum dependence. If the Hamiltonian is

$$H = V_1(p) + V_2(q) \sum_{n=-\infty}^{\infty} \delta(t - n),$$

the quantum map is

$$U_{n,n'} = \frac{1}{N} \exp(-2\pi i N V_2(\frac{n+a}{N})) \sum_{m=0}^{N-1} \exp(-2\pi i N V_1(\frac{m+b}{N})) \exp(\frac{2\pi i}{N}(m+b)(n-n')) \quad (3.6)$$

For the map used below we have taken  $V_1(p) = -g_1 \cos(2\pi p)/(2\pi)$  and  $V_2(q) = -g_2 \cos(2\pi q)/(2\pi)$ . If  $(a = b = 1/2)$ , this once again ensures special symmetry properties of the quantum map, a case we call below the symmetric Harper map. We can retain time reversal and break parity by choosing  $b = 1/2$  and  $a \neq 1/2$ , and or break both symmetries. The classical map is  $(q_{t+1} = q_t + g_1 \sin(2\pi p_{t+1}), p_{t+1} = p_t - g_2 \sin(2\pi q_t))$ , again the mod 1 rule is assumed. If  $g_{1,2}$  are equal, as assumed in this paper, the transition to chaos occurs around  $g_{1,2} = 0.63$ . In both the kicked Harper model and the rotor the time between kicks has been taken as unity, as anyway there are two parameters in the quantum problem, the scaled Planck constant  $N$  and the kick strength ( $K$  or  $g$ ).

The bakers map [11,12] comes in several varieties. It has been shown that the usual bakers map  $((q_{t+1} = 2q_t, p_{t+1} = p_t/2)$  if  $0 < q_t < 1/2$  and  $(q_{t+1} = 2q_t - 1, p_{t+1} = (p_t + 1)/2)$  if  $1/2 < q_t < 1$ ) is isomorphic to the  $(1/2, 1/2)$  Bernoulli process. The quantum bakers map on the torus is then the unitary operator

$$U = G_N^{-1} \begin{pmatrix} G_{N/2} & 0 \\ 0 & G_{N/2} \end{pmatrix}, \quad (3.7)$$

where  $G_N$  is the finite Fourier transform matrix with elements

$$(G_N)_{m,n} = \frac{1}{\sqrt{N}} \exp(-2\pi i(m + 1/2)(n + 1/2)/N).$$

We have assumed anti-periodic boundary conditions  $(a = b = 1/2)$  and this is known to preserve classical symmetries of the usual bakers map.

The generalized bakers map used in this paper is a dynamical system implementing the  $(2/3, 1/3)$  Bernoulli process and is the classical map  $((q_{t+1} = 3q_t/2, p_{t+1} = 2p_t/3)$  if  $0 < q_t < 2/3$  and  $(q_{t+1} = 3q_t - 2, p_{t+1} = (p_t + 2)/3)$  if  $2/3 < q_t < 1$ ). The quantum map is the unitary operator

$$U = G_N^{-1} \begin{pmatrix} G_{2N/3} & 0 \\ 0 & G_{N/3} \end{pmatrix}. \quad (3.8)$$

#### IV. NUMERICAL RESULTS

Time dependent quantum chaotic systems such as the kicked rotor on the cylinder are known to suppress classical chaos and lower diffusion [3]. The corresponding suppression in the case of bounded systems could be the average relaxation such as measured by  $\langle c \rangle$ . We note that the sum over  $n$  and  $n'$  expressing the average can be factored into two single sums, and we see that if for instance we had a parity symmetry forcing the wavefunction to be essentially identical in the subspaces  $A$  and  $B$  we would have  $\langle c \rangle = 1$ , which is indeed the case for the fluctuations shown in Fig. 1. The average  $\langle c \rangle$  could also be greater than unity in the presence of symmetries, or if the partition  $B$  is identical to  $A$ .

Fig. 2a shows the average for the quantized baker map implementing the Bernoulli scheme  $(2/3, 1/3)$  as a function of the inverse Planck constant  $N$ . The partitions are such that  $f_A = f_B = 1/2$ . Shown is the deviation of the average from unity and an approximate power law is observed for large  $N$ . Thus we can write

$$\langle c \rangle \sim 1 - \alpha N^{-\gamma}, \quad (4.1)$$

and in this case  $\gamma \approx 3/4$ . The relaxation localization is implied by  $\alpha$  being positive. Fig. 2b shows the same quantity for the symmetric standard map and we find for the partition  $f_A = 1/4, f_B = 3/4$  that  $\gamma \approx 1$ , with a different value of  $\alpha$ . We note that in both the cases there is a small oscillation about the fitted straight line. Further results, especially on the variation of the average with the parameters of chaos, are in ref. [8].

Fig. 3 shows the standard deviation  $\sigma$  scaled to  $\sigma N$  as a function of the kick strength in the case of the symmetric standard map. The transition to classical chaos at  $K \approx 1$  is visible in the variance of the fluctuations as a point at which it attains an approximately constant value. The relaxation fluctuations are therefore significantly different depending on the dynamical nature of the classical limit, being in general larger for regular systems than chaotic ones, and thus provide a novel diagnostic device for the study of quantized chaotic systems. Further results may be found in ref. [8]. Here we will turn to a more closer appraisal of the ingredients of the variance itself.

In a slight modification of the equation for the variance, define

$$S = 2 \sum_{m_2 > m_1} \left| \sum_{n=n_0}^{n_0+l-1} \langle n | \psi_{m_2} \rangle \langle \psi_{m_1} | n \rangle \right|^4. \quad (4.2)$$

The quantity  $S$  is simply related to the variance of the fluctuations. The relevant partitions have been generalized slightly so that  $P_A = \sum_{n=n_0}^{n_0+l-1} |n\rangle\langle n|$  and the classical partition is the vertical rectangle of length  $l/N$  whose origin is at  $n_0/N$ . The  $B$  partition is the complementary space.  $S$  is potentially a function of  $l$ ,  $N$  and  $n_0$ . For generic systems the origin  $n_0$  should not play a role and we will expect this dependence to drop out. In fact the case of the symmetric standard map when the partition is constructed from the position basis is a counter-example to this statement. But what we will go on to establish is that for generic quantum chaotic systems and generic partitions,  $S$  is asymptotically (large  $N$ ) only a function of  $f = l/N$  and that the functional dependence is determined by time reversal symmetry.

In Fig. 4a is plotted the behaviour of  $S$  for the symmetric standard map and the dependence on  $n_0$  is clearly visible as the non-analyticity as a function of the fraction  $f$ . On the other hand Fig. 4b illustrates a smooth functional dependence independent of  $n_0$  when the parity symmetry is broken by choosing  $a = 0.35$  instead of 0.5. The universality of this curve has been checked against other models such as the kicked Harper map. In the next section a form of this smooth function is derived within the framework of RMT. Fig. 5 consolidates three cases of the kicked Harper map. The function  $S$  with both parity (R- symmetry) and time-reversal, with just time-reversal and the case when there is neither parity nor time-reversal symmetry. The fluctuations clearly distinguish these situations and illustrates the intuitive expectation that the fewer the symmetries the smaller would be the fluctuations about the “quantum equilibrium”.

## V. FLUCTUATIONS ACCORDING TO RMT

Random Matrix Theory [13] has been quite successful in the description of many aspects of complex quantum systems. It is natural to expect that the fluctuations be also described adequately within this theory. Already work on the survival probability has been dealt using RMT with success. The fluctuations studied above are characterized by certain higher order correlations between eigenfunctions and the evaluation of these within the RMT framework for the case of time reversal symmetric generic systems is dealt with here.

The appropriate ensemble of matrices is the circular orthogonal ensemble, but we will equivalently use the Gaussian orthogonal ensemble (GOE). Thus in the spirit of RMT (and statistical mechanics) we will equate any quantity with its ensemble average. Thus when  $\text{Tr}(P_A) = l = fN$  we get

$$\langle c \rangle = \langle \langle \frac{1}{Nf(1-f)} \sum_{m=0}^{N-1} \sum_{n=0}^{l-1} \sum_{n'=l}^{N-1} |\langle n | \psi_m \rangle|^2 |\langle n' | \psi_m \rangle|^2 \rangle \rangle. \quad (5.1)$$

The double bracket represent average over the ensemble. GOE for eigenfunctions is particularly simple with the assumption that each vector covers an  $N$  dimensional sphere uniformly. More details that are crucial to the following can be found for instance in [13].

Thus under the assumption that there are no favoured eigenfunctions we get

$$\langle c \rangle = \frac{l(N-l)}{f(1-f)} \langle \langle |\langle n | \psi_m \rangle|^2 |\langle n' | \psi_m \rangle|^2 \rangle \rangle \quad (5.2)$$

We change to a different notation purely for the sake of convenience. We denote the the  $n - th$  component of the vector  $\lambda$  by  $x_{n\lambda}$ . Then using the result [13]

$$\langle\langle x_{i\lambda}^2 x_{j\lambda}^2 \rangle\rangle = \frac{1}{N(N+2)} \quad (5.3)$$

we get

$$\langle c \rangle = \frac{N}{N+2} \sim 1 - 2/N. \quad (5.4)$$

The final approximation is for large values of  $N$  (the classical limit). We see that this is consistent with our simulations for the average value of the fluctuations. It predicts that for generic systems the average is less than unity and that the leading correction is proportional to  $\hbar$ . This agrees with our result for the standard map but the bakers map has a different behaviour as the leading correction was found to be of order  $\hbar^{3/4}$ . This is consistent with what has been observed by others so far: that the quantum bakers map is somewhat “less random” than other models of quantum chaos [14].

The variance is calculated in a similar manner, but leads to higher order correlations that appear to be a pure “two-vector” result in comparison to that used for the average. Any two eigenvectors of the ensemble are correlated due to the requirement of orthonormality and the full derivation of the reduced densities is not known to the author at present. Nevertheless much can be derived about the variance. Concentrating on  $S$  (which is trivially related to the variance) we get

$$S = \langle\langle 2 \sum_{m_2 > m_1} \left| \sum_{n=n_0}^{n_0+l-1} \langle n | \psi_{m_2} \rangle \langle \psi_{m_1} | n \rangle \right|^2 \rangle \rangle \quad (5.5)$$

or

$$S = N(N-1) \langle\langle \left| \sum_{n=1}^l x_{n\lambda} x_{n\mu} \right|^2 \rangle \rangle \quad (5.6)$$

We have made use of the fact that GOE eigenvectors are real and we also require in the above that  $\lambda \neq \mu$ . We have also dropped the  $n_0$  term (or set it equal to unity) as the statistical theory does not distinguish between eigenvectors. It is clear therefore that  $S$  is a measure that may be called “incomplete orthonormality”, while the average is related to “incomplete orthogonality”.

The sum over  $l$  terms is equal (due to orthonormality) to a sum over  $N - l$  terms and therefore statistically we derive that

$$S(l) = S(N - l) \quad (5.7)$$

where we have explicitly written the dependence of  $S$  on  $l$ . We must note that this is not an exact condition of symmetry (from detailed dynamics) as is apparent from the numerical results, but is exact within the framework of RMT. The deviations from this symmetry could therefore provide an interesting measure of deviation from statistical behaviour.

Further expansion of the fourth power in the equation of  $S$  and book-keeping leads to the following fourth order polynomial for  $S$ .

$$\frac{S(l)}{N(N-1)} = a_1 l + a_2 l(l-1) + 6a_3 l(l-1)(l-2) + a_4 l(l-1)(l-2)(l-3) \quad (5.8)$$

and

$$\begin{aligned} a_1 &= \langle\langle x_{i\lambda}^4 x_{j\lambda}^4 \rangle\rangle, \\ a_2 &= 3 \langle\langle x_{i\lambda}^2 x_{j\lambda}^2 x_{i\mu}^2 x_{j\mu}^2 \rangle\rangle + 4 \langle\langle x_{i\lambda}^3 x_{j\lambda}^3 x_{i\mu} x_{j\mu} \rangle\rangle, \\ a_3 &= \langle\langle x_{i\lambda}^2 x_{j\lambda}^2 x_{i\mu} x_{j\mu} x_{i\nu} x_{j\nu} \rangle\rangle, \\ a_4 &= \langle\langle x_{i\lambda} x_{j\lambda} x_{i\mu} x_{j\mu} x_{i\nu} x_{j\nu} x_{i\alpha} x_{j\alpha} \rangle\rangle. \end{aligned} \quad (5.9)$$



These are truly two-vector averages (  $i$  and  $j$  indices can be also thought of as denoting vectors rather than components). None of the indices must be the same in each of the above expressions. We see quite easily that

$$a_4 = 3a_3/(3 - N). \quad (5.10)$$

This follows on summing over the index  $\lambda$  in the expression for  $a_4$  and using orthonormality. Further we have that

$$(N - 1) \langle\langle x_{i\lambda}^3 x_{j\lambda}^3 x_{i\mu} x_{j\mu} \rangle\rangle = - \langle\langle x_{i\lambda}^4 x_{j\lambda}^4 \rangle\rangle. \quad (5.11)$$

This follows from summing over the index  $\mu$ .

Further using the symmetry in the form of  $S$  gives

$$a_1 + (N - 1)a_2 + 3(N - 1)(N - 2)a_3 = 0 \quad (5.12)$$

Thus putting together this information leads to

$$\frac{S(f = l/N)}{N(N - 1)} = f(1 - f) \left[ \frac{a_1 N^2}{(N - 1)} - N^2(N - 1)a_4 \right] + f^2(1 - f)^2 a_4 N^4. \quad (5.13)$$

The symmetry about  $f = 1/2$  is now obvious.  $a_1$  can be evaluated exactly using the methods in [13] and gives

$$a_1 = 9/(N(N + 2)(N + 4)(N + 6)) \sim 9/N^4. \quad (5.14)$$

The correlation  $a_4$  is unfortunately beyond the author, but it is sufficient to observe that

$$a_4 \sim 3 \langle\langle x_{i\lambda} x_{j\lambda} x_{i\mu} x_{j\mu} \rangle\rangle^2 = 3/N^6 \quad (5.15)$$

The corrections to this are of order  $N^{-7}$ . The factor 3 is necessary as the number of different ways of choosing 2 indices from 4 is 6 and choosing any two results in the automatic choice of the other pair. This new two-vector correlation is easy to evaluate ( [13]) and we get the above result.

Collecting all the correlations we finally arrive at

$$S(f = l/N) = 3f^2(1 - f)^2 + O(N^{-1}) \quad (5.16)$$

Thus we have proved that  $S$  is only a function of  $f$  in the large  $N$  limit. This functional form should match those for time-reversal symmetric systems with no special symmetries. This is illustrated in Fig. 6, and the fit is satisfactory. The standard deviation of the fluctuations is for such systems thus given simply by

$$\sigma = \sqrt{3}/N + O(N^{-2}), \quad (5.17)$$

and implies the independence of the width of the fluctuations from the size of the partitions. In contrast the numerical results show a strong  $f$  dependence for systems with special symmetries such as parity [8]. Further work is underway for elucidating features of the time-reversal breaking case as well.

## VI. SUMMARY

We have studied correlations between operators in quantum chaotic systems. The relaxation towards an oscillatory state of decorrelation or “equilibrium” has been analysed numerically and also from the point of view of RMT. Certain universal features have been found and in the case of time-reversal symmetric systems these have been derived using RMT.

There are many natural extensions to this work, the most important being consideration of general density operators rather than projectors. Further it has been found in [8] that the relaxation process is Gaussian implying that the mean and standard deviation characterise the process completely. The question of energy has not arisen in this work

because of our models. Therefore the generalization of this work to Hamiltonian flows with infinite Hilbert spaces is of considerable importance. Connections have to be made between these approaches in quantum chaos and the existing methods of quantum statistical mechanics.

The effect of scarring of wavefunctions by classical periodic orbits tends to localize many quantum states. It would be of interest to see if the measures defined herein are sensitive to this phenomenon. We have already noted deviations from RMT in the case of the quantized bakers map which is known to have a large number of scarred eigenstates.

---

\* e-mail: arul@prl.ernet.in

- [1] V. I. Arnold and A. Avez, *Ergodic Problems of Classical Mechanics* WA Benjamin, New York (1968).
- [2] S. Weigert in *Adriatico Research Conference and Miniworkshop, Quantum Chaos*, edited by H. A. Cerdeira, R. Ramaswamy, M. C. Gutzwiller and G. Casati (World Scientific, 1990).
- [3] F. M. Izrailev, Phys. Rep. **196**, 299 (1990).
- [4] Y. Elskens and R. Kapral, J. Stat. Phys. **38**, 1027 (1985).
- [5] P. Gaspard, J. Stat. Phys. **68**, 673 (1992).
- [6] O. Bohigas, S. Tomsovic, and D. Ullmo, Phys. Rep. **233**, 45 (1993).
- [7] A. Lakshminarayan, and N. L. Balazs, J. Stat. Phys. **77**, 311 (1994).
- [8] A. Lakshminarayan, Phys. Rev. E. **56**, 2540 (1997) (chao-dyn/9704001).
- [9] F. Leyvraz *et. al.*, Phys. Rev. Lett. **67**, 2921 (1991); Y. Alhassid and N. Whelan, Phys. Rev. Lett. **70**, 572 (1993); A. Tameshtit and J. E. Sipe, Phys. Rev. A **45**, 8280 (1992); J. Wilkie and P. Brumer, Phys. Rev. Lett. **67**, 1185 (1991).
- [10] P. Leboeuf *et. al.*, Phys. Rev. Lett. **65**, 3076 (1990).
- [11] N. L. Balazs, and A. Voros, Ann. Phys. (N. Y.) **190**, 1 (1989).
- [12] M. Saraceno, Ann. Phys. (N.Y.) **199**, 37 (1990).
- [13] T. A. Brody, *et. al.* Rev. Mod. Phys., 53 385 (1981).
- [14] P. W. O'Connor, S. Tomsovic, and E. J. Heller, Physica **55D**, 340 (1992).
- [15] S.J. Chang, and K. J. Shi, Phys. Rev. Lett. **55**, 269 (1985).

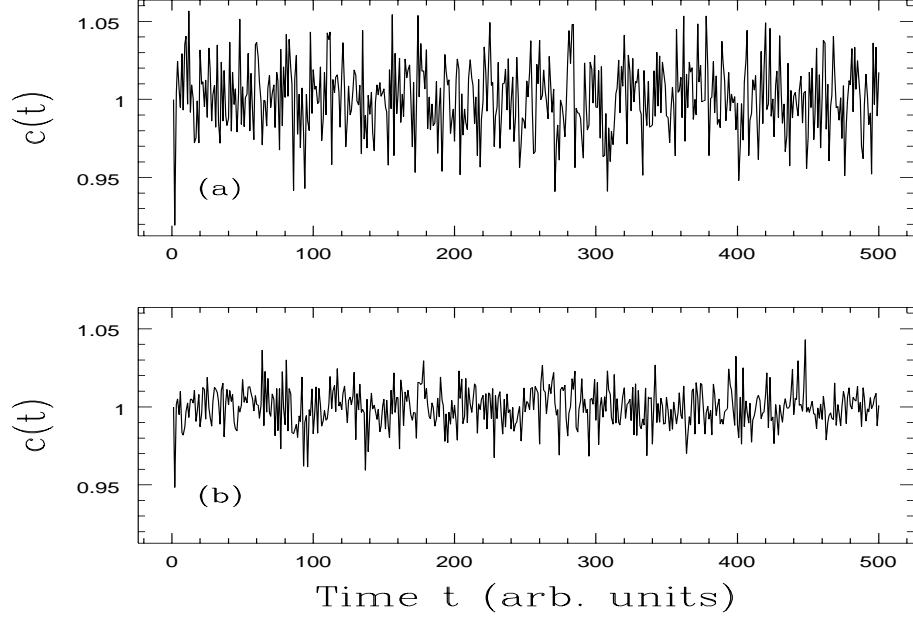


FIG. 1. The relaxation fluctuations as a function of time for the symmetric standard map with  $K = 20$  and (a)  $N = 100$  (b)  $N = 200$ .

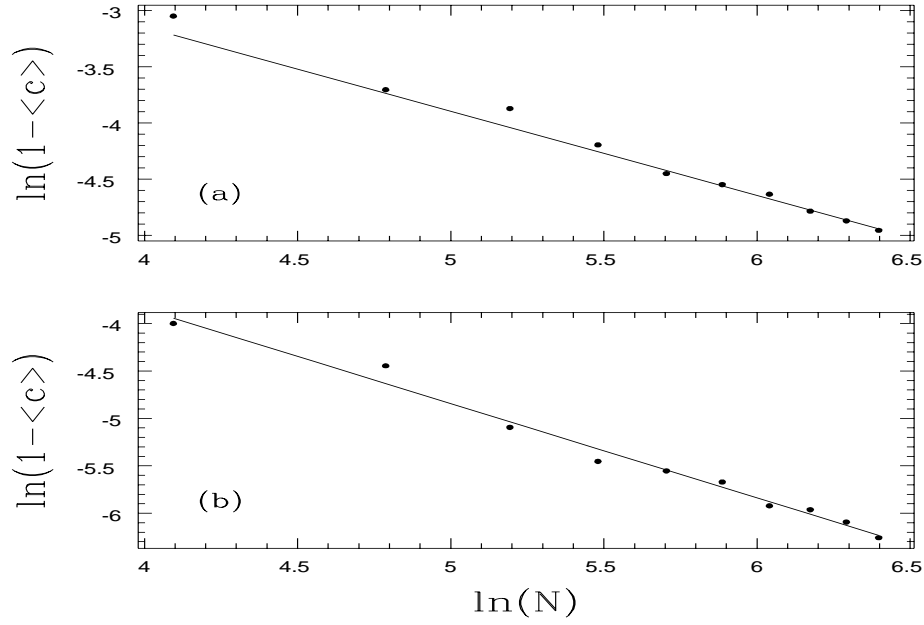


FIG. 2. The average of the fluctuations for (a) the quantum baker's map quantizing the  $(2/3, 1/3)$  Bernoulli scheme and (b) the standard map with  $K = 20$ . Shown is the logarithm of the deviation from unity as a function of  $\log(N)$ .

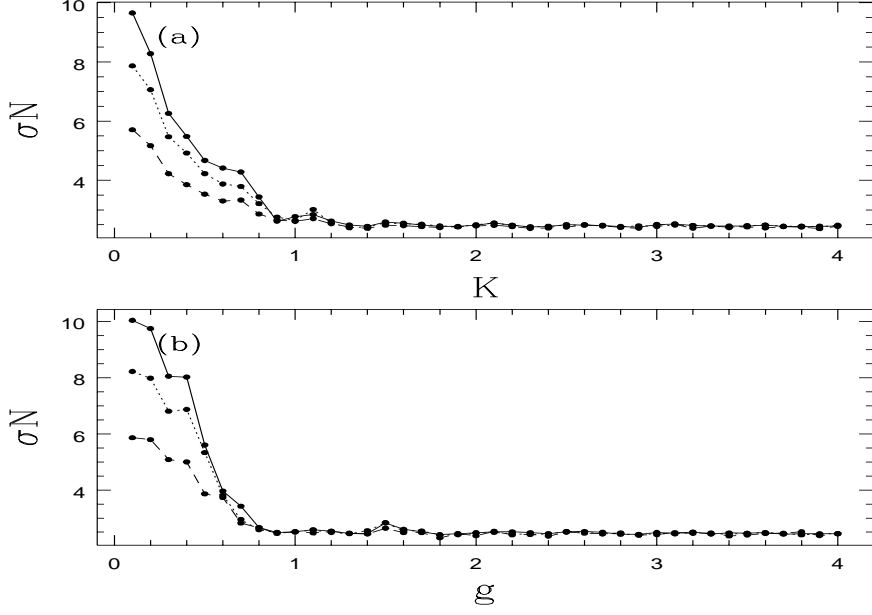


FIG. 3. The scaled standard deviation  $\sigma N$  as a function of the kick strength for (a) the symmetric standard map, (b) the symmetric Harper map. The solid line corresponds to  $N = 300$ , the dotted line to  $N=200$  and the dashed line to  $N=100$ .

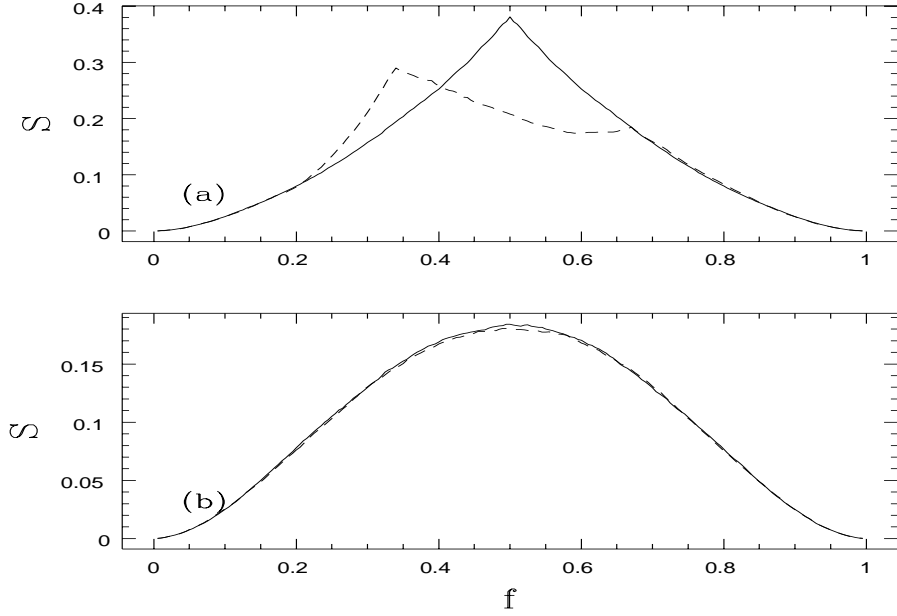


FIG. 4. The eigenfunction sum  $S$  as a function of  $f$ . (a) The symmetric standard map with  $N = 200$ , the solid line is when  $n_0 = 0$  and the dashed one for  $n_0 = 66$ . (b) Case of the asymmetric standard map with  $(a = 0.35, b = 0.0)$ , the solid line is when  $n_0 = 0$  and the dashed one for  $n_0 = 66$ . In all cases  $K = 20$ .

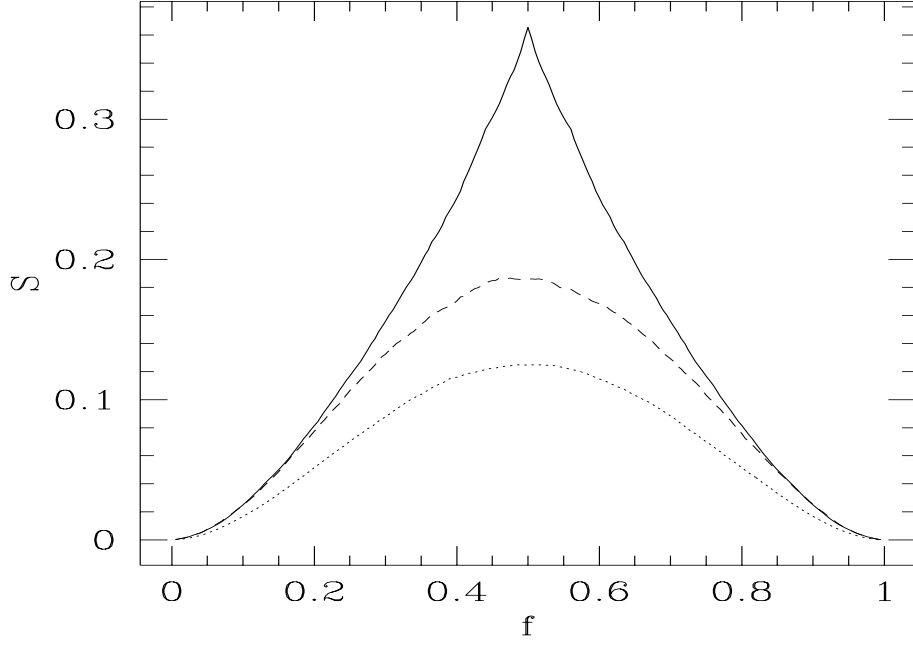


FIG. 5. The eigenfunction sum  $S$  for the Harper map with  $g = 8$ . The symmetric Harper map with  $(a = 1/2, b = 1/2)$  is the solid line while the case  $(a = 0.35, b = 1/2)$  is the time-reversal symmetric case with no special phase space symmetries and the dotted line  $(a = 0.35, b = 0.35)$  breaks also time-reversal symmetry. In all cases  $N = 200$ .

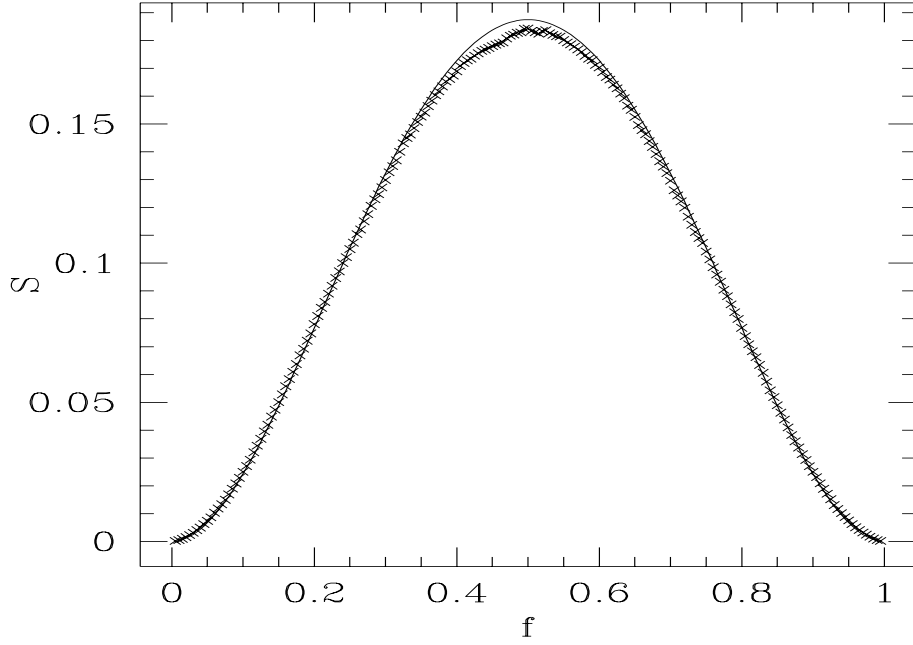


FIG. 6. Comparison of the prediction from RMT, the solid line, with the asymmetric standard map ( $N=200, K=20, a=0.35, b=0$ ), the crosses.